RECONSTRUCTION OF HEAD-TO-BONNET TOP IMPACT IN CHILD PEDESTRIAN-TO-PASSENGER CAR CRASH

Jianfeng Yao[1], Jikuang Yang[1], Dietmar Otte[2], Rikard Fredriksson[3]
[1]Chalmers University of Technology, Sweden
[2]Medical university Hanover Accident Research Unit, Germany
[3]Autoliv Research, Sweden

ABSTRACT

A real world child pedestrian accident was reconstructed using multi-body system (MBS) model, facet model and FEM model respectively to investigate the head impact biomechanics and injury mechanism during the accident. Child headform impact tests were carried out to acquire the mechanical properties of vehicle front at the head and hip impact locations in the accident. The overall kinematics of pedestrian and head impact condition in each reconstruction are quite similar and close to those values in the accident. The calculated head injury parameters are on the same level and correspond well to the injury outcomes in the accident. Nevertheless, minor variations of these values still exist due to different numerical methods.

Keywords: Child pedestrian, accident reconstruction, head injury, numerical simulation

CHILDREN (0-15 YEARS OLD) were most frequently involved in the pedestrian accidents. In USA, nearly 30% of pedestrian accident victims were children (FARS 1995-2002). This value varies in different countries: 33.4% in Germany, 34.2% in Japan, 25.9% in Australia (IHRA, 2001), and 42.5% in Saudi Arabia (Al-Ghamdi, 2002). In the child pedestrian accident, head injuries are most common and usually the leading cause of death (EEVC, 1982). In a study based on the accident data from Australia and Germany, Fildes et, al (2004) proposed to reduce the head/bonnet injuries as the top priority in the child pedestrian crashes. However, this requires a better understanding of the head impact dynamics and injury mechanisms in the child pedestrian accident.

During the past three decades significant reductions in pedestrian fatalities have been achieved in Europe, Japan and the United States (CARE, 2004; JTSP, 2004; FARS, 2004). At the mean time, the vehicles experienced notable changes with smoother front-end shape, recessed bonnet leading edge and bumper leading edge, laminated windscreens and increasing use of anti-lock braking systems. So far there is no direct statistical study to prove that injury reduction is achieved by these changes, however, an analysis of the pedestrian accident cases in GIDAS and IHRA database showed that a potential of 18%-27% reduction of serious injuries could be achieved by improving current vehicle designs (Berg, et al, 2002).

To understand the injury mechanism in the pedestrian accident and improve car front design, it requires detailed information about the dynamic responses and injury biomechanics of pedestrians during the impact. The component impacts such as proposed by EEVC (2001) are not suitable to monitor the kinematics and the overall injury risk of an impacted pedestrian. The results may be misleading and even conflicting for different height groups. On the other hand full-scale dummy test show a more realistic kinematics but not well reproducible. Thus it is obvious that an advanced numerical simulation procedure is needed.

The object of this paper is to investigate the pedestrian injury mechanism by reconstructing the real world pedestrian accident using numerical simulation procedures. Three different numerical methods including multibody model, facet model and finite element model were used to reconstruct a real world child pedestrian accident. The reconstruction results were correlated with the injury outcomes in the accident. The head injury was the main focus since it's the current research priority.

METHOD AND MATERIALS

ACCIDENT CASE COLLECTION: A study of pedestrian accidents is carrying out in a co-operation between CHALMERS University and Hanover Medical University. The aim is to understand the pedestrian injury mechanism by accident reconstructions and therefore provide useful information for the car front design. The pedestrian accident cases were collected both in Sweden (Yang, 2003) and Germany (Otte, 1998). These accidents were then selected for accident reconstructions based on certain criteria such as car model year, injury severity, impact speed, age group and etc.

For each collected case, detailed information regarding pedestrians, vehicles, and crash environment was documented by the accident investigation team that is composed of medical doctor, biomechanical engineer and research expert. Injuries sustained by each pedestrian were coded according to AIS 90. The anthropometric data of pedestrian such as age, gender, height, and weight were registered in the hospital. Accident witnesses were investigated to obtain the accident information such as pedestrian posture, impact direction and etc.

The vehicles involved in the accidents were recorded with detailed information about car maker, model year, and estimated impact speed. The deformation pattern, contact points on the car and characteristics of traces on the road were measured and marked in a 3-dimensional x, y, z –coordinate system. Pictures of impact locations are taken and could be used for analysis. The final positions of the pedestrian, car and any other related features were also recorded. These collected information provided most important data to carry out the accident reconstructions.

In this paper, a child pedestrian accident case was selected for reconstruction using different numerical methods.

SELECTED ACCIDENT CASE FOR RECONSTRUCTION: A passenger car-to-child pedestrian accident case was selected for reconstruction. The driver claimed that he saw a group of children playing on the right side of the road from about 50 meters away (Position A in Figure 1a). When the car was approaching the group of children at speed about 70 km/h, the driver lifted his foot from the accelerator as he noticed the potential risk. Then he began to brake slightly as the car approaching the cross. Suddenly a 7-year-old boy began running across the street when the car arrived at position B. The driver braked hardly and manipulated the car to avoid an impact.

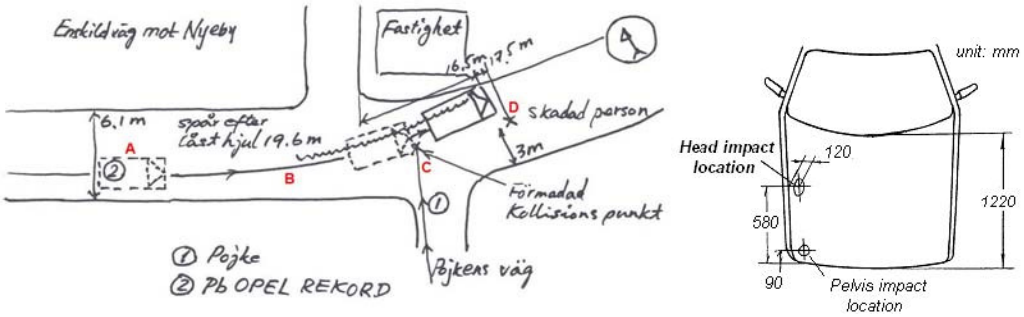

(a) **(b)**

Fig. 1-Drawing of (a) accident scene (b) the location of head and pelvis impact on the car

The car, however, still hit the child by the right front corner at position C at an estimated speed about 40 – 45 km/h. The car stopped about 10 meters away from C, and threw the child to position D (Figure 1a).

The child sustained unconsciousness due to the head-brain injuries: fracture at left orbit (AIS 3), subdural hematoma at left frontal lobe (GCS 5, GOS 2, and AIS 5). Except some slight outer skin injuries in the lower extremities, no other injuries were reported. After 7 weeks the child could stand up but not walk. The damage of the accident car and interactions between the car and body segments of the child were determined. The right headlight of the accident car was broken. Two dents were

found on the hood. The contact dents were visible on the leading edge of the hood and the hood top. The dent on the hood top was identified as the result of the head impact. Its center was about 580 mm away from hood edge and 120 mm away from right fender. Another dent caused by the pelvis impact, was about 90 mm away from the hood leading edge. No evidence indicated the damage to the structures beneath the hood. The measured wrap around distance (WAD) was 1350 mm. The throw distance was 14 m from initial impact.

HEADFORM IMPACTOR TEST: The headform impact test was carried out to obtain the car front stiffness at the head and pelvis impact locations in the accident (Figure 2). The test vehicle has the same maker, model and series as the accident car. The child headform used was the standard EEVC child pedestrian headform which consists of an aluminum sphere and covered by a 11mm thick vinly skin. The total weight of the headform is 2.5 kg and the diameter is 130 mm. The headform was equipped with an accelerometer at the center of sphere and sampling the data at frequency of 10,000 Hz. During the test, the headform was propelled to hit the hood top at an angle perpendicular to the hood. The impact speed was set to 30 km/h.

Fig. 2-Headform impact test (a) Dents on the accident car (b) Dents on the test car

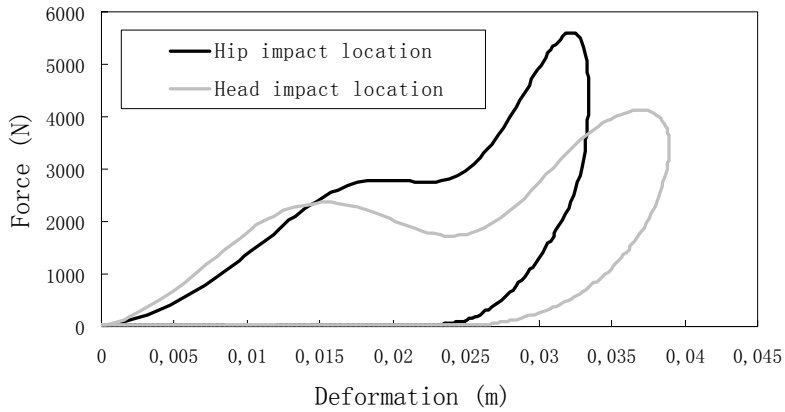

Fig. 3-Force-deformation characters of two impact locations on the hood

The force-deformation characteristics at these two locations were then calculated based on the acceleration history. Two assumptions were made for the calculation: the headform is rigid and it has no rotational motion during the impact. It was observed that the deformation of the headform skin is quite small and neglectable if compared with the deformation of the vehicle hood. The headform has no noticeable rotational motion during the impact since the impact angle was perpendicular to the hood. Thus these two assumptions were satisfied. The resulting force-deformation characteristics are shown in Figure 3.

VEHICLE MODEL DEVELOPMENT

Multi-body system (MBS) model: A MBS vehicle model was developed based on the drawings of the production car that had the same make, model and series as the accident car. The vehicle front structures were represented by four ellipsoids: lower bumper, bumper, hood edge and hood top. Several planes and ellipsoids were assigned to describe the rear part and the wheels. The force-deformation properties of the hood and hood edge were obtained from the headform impactor test. The bumper stiffness was defined according to EuroNCAP test results of a similar car.

FEM and facet car models: A FEM car model is generated also based on the production car geometry drawings and the under hood structures. The FEM car model includes lower bumper, bumper, hood edge, lamp, hood, inner hood, under hood structures, windscreen, fender and wheel. To reduce the computation time, the rear parts of the car were not modeled since they did not contact with pedestrian in the accident. Proper material properties were assigned to different parts. The resulting mesh consists of 31,986 elements and 30,732 nodes.

The facet car model was generated based on the FEM car model. The structures underlying the outer surface such as inner hood and the under hood structures were deleted. Null material properties were assigned to all parts, which is named as facet mesh in MADYMO. The stiffness of the facet surface was defined using force-deformation functions. The final mesh consists of 23,714 elements and 24,051 nodes. The completed mesh is rigid which accurately describes the outer surface while still allows a fast computation.

Validation of car models: The MBS, FEM and facet car models were validated by reconstruction of headform tests on the hood top and hood edge according to the impact test conditions. The ellipsoid, FEM and facet child headform models from MADYMO database were used respectively in the simulations, as shown in Figure 4 for the validation of FEM car model for example. The simulated headform acceleration was compared with the acceleration in the tests. The magnitude and pulse duration of headform acceleration in the simulations are similar to those in the test (Figure 5).

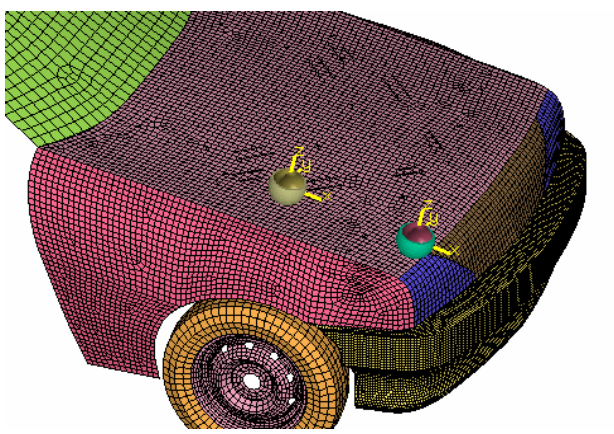

Fig.4-Reconstruction of headform impactor test for FEM car model

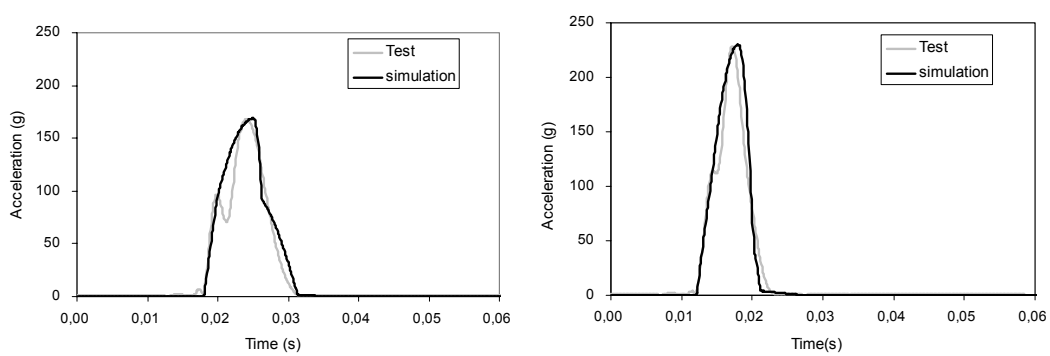

(a)

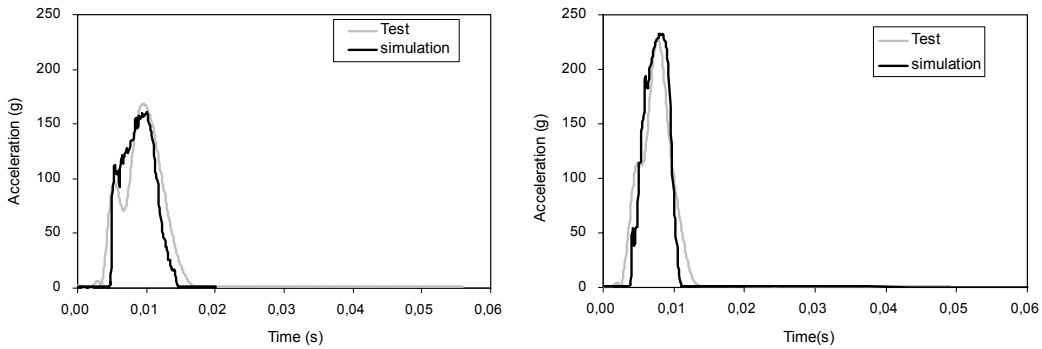

(b)

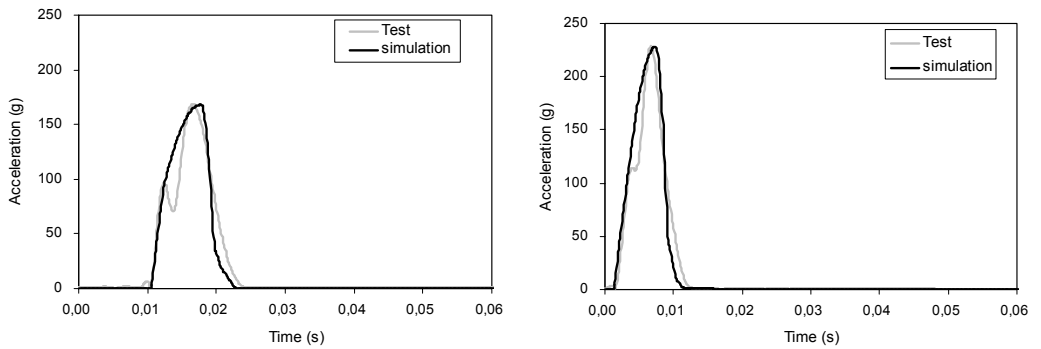

(c)

Fig. 5- Validation of hood stiffness of (a) MBS car model (b) FEM car model (c) Facet car model

CHILD PEDESTRIAN MODEL DEVELOPMENT

Multi-body system (MBS) model: A 7-year-old child pedestrian MBS model was scaled down from a validated adult model (Liu and Yang, 2002; Yang et al, 2000). The GEBOD program (TNO, 2003) was used to generate the mass/inertial properties and characteristic dimensions of various body segments based on the anthropometric information of the child victim such as age, height, and weight. The joint properties and contact stiffness of the body segments are defined by scaling method. The model consists of 15 ellipsoids representing head, neck, chest, abdomen, hip, upper and lower extremities and connected by 14 spherical joints.

Facet child pedestrian model: In the contacts between an ellipsoid and a facet surface, if the penetration is too large, it will cause a sudden change in the magnitude and direction of the contact force. This is the common case in the simulation of child pedestrian to car impact since the dimension of ellipsoids representing upper and lower extremities is quite small. To improve the contact property, the child pedestrian was also modeled by facet elements.

The facet child pedestrian model was generated from the MBS child pedestrian model. The meshes were converted from the original ellipsoids. The same joint properties and contact stiffness as the MBS model were used in the facet model.

RECONSTRUCTION SETUP: The setups for the three numerical simulations are identical. The initial posture of child pedestrian was set to be running in the direction perpendicular to the car moving direction. The running speed was estimated at 10 km/h. The friction coefficient between child body segments and road surface was set to 0.6 based on empirical data. The friction coefficient between the wheels and road surface was assumed to be 0.7. The diving angle was assumed as 2 degrees. Steering effect was also simulated by defining an angular velocity of 1 rad/sec about z-axis whose origin was at the center of the curvature of skid marks. The initial speed of the car was set to 40 km/h.

RESULTS

KINEMATIC RESPONSE: The kinematic response of the reconstructed child pedestrian was evaluated using the car damage information, measured throw distance and wrap around distance from the accident investigation.

The first 80 ms of primary impacts in three numerical simulations are depicted in Figure 6. The general kinematics of child pedestrians are quite similar in all three reconstructions, however, small differences still exist. At t=80 ms, the pedestrian heads in the reconstructions with MBS car model and facet car mode are almost parallel to the hood top while the head in the reconstruction using FEM model have an obvious downward angle.

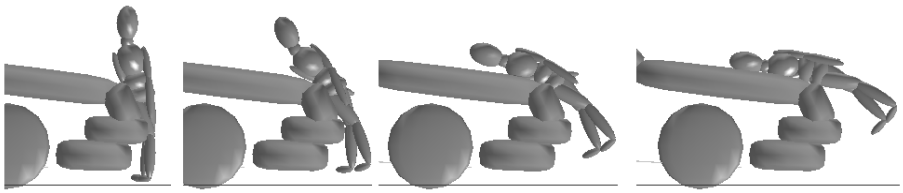

(a) MBS car model and MBS pedestrian model

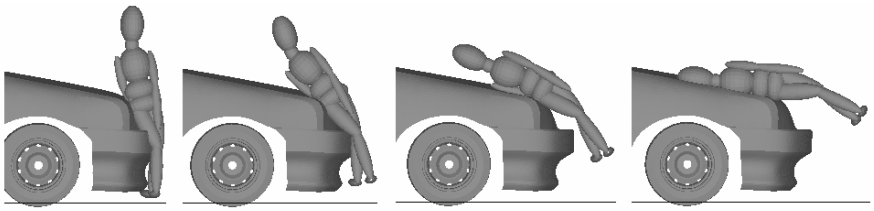

(b) Facet car model and facet pedestrian model

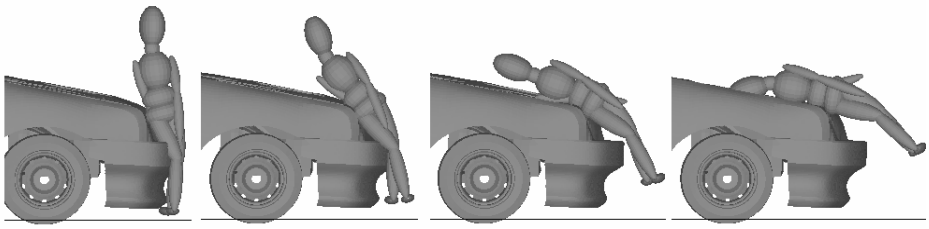

(c) FEM car model and facet pedestrian model

Fig. 6- Kinematics of 7-year-old child in the collision (20-80 ms, Δt=20 ms)

The throw distance and wrap around distance in the reconstructions are measured and listed in Table 1. These values are quite close to the values measured in the accident investigation.

Table 1. Throw distance and wrap around distance in the reconstructions

	Throwing distance (m)	Wrap around distance (m)
MBS model	13.5	1.32
Facet model	13.6	1.33
FEM model	13.3	1.30
Accident	14	1.35

HEAD IMPACT CONDITIONS: The head impact conditions were described in terms of impact angle, impact speed and impact timing. The results from reconstructions are presented in Figure 7.

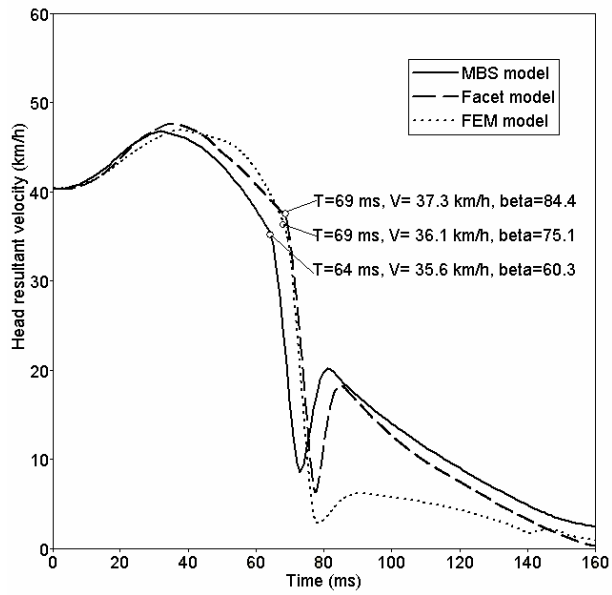

Fig.7- The time history of the head resultant velocity with respect to the car front

CALCULATED HEAD INJURY PARAMETERS: The calculated head injury parameters are summarized in Table 2, in terms of peak 3ms head acceleration, HIC value, head angular velocity and angular acceleration. Figure 8 shows the time history of the head acceleration in three different numerical simulations.

Table 2. Calculated head injury parameters

	3ms acc. (g)	HIC_{15}	Angular Vel. (rad/s)	Angular Acc. (rad/s^2)
MBS model	122	1391	68	6868
Facet model	146	1865	76	9056
FEM model	126	1275	59	9358
Mean	131	1520	68	8427

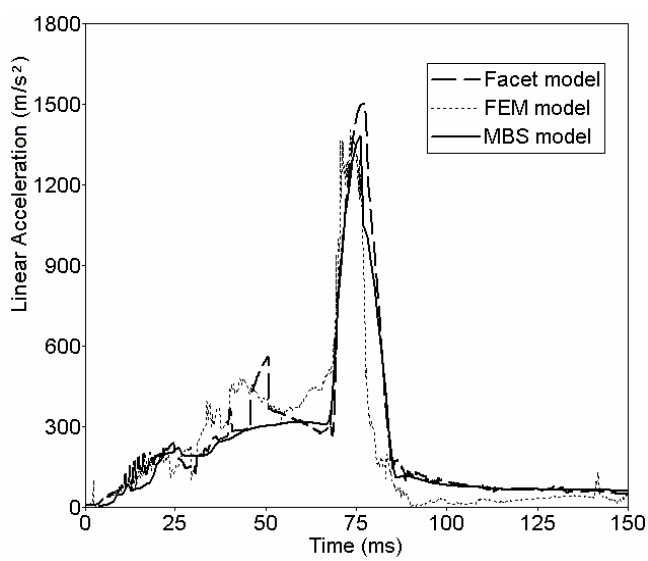

Fig.8- Head acceleration curve in three numerical simulations

EFFECTIVE HEAD MASS: Unlike the free-flight headform in the impactor test, the pedestrian head in the accident collision is restrained by the neck. This restraint force applied by the neck could be divided into two vectors : one is colinear with the impact force applied by the hood and another one is perpendicular to the impact force. The collinear force could affect the impact between the head and the vehicle hood, which could be regard as adding or reducing a mass from the head.

The effective mass of the head could be defined as following.

$$m_{eff} = \left[\int_{t1}^{t2} F dt\right] \div \left[\int_{t1}^{t2} a dt\right] \quad (1)$$

Where t_1 is the time when head impacts against hood and t_2 is the time when head left hood. F and a are the head impact force and acceleration during the impact process against hood.

The m_{eff} is an important parameter since it reflects the effective head mass during the head impact. In the simulation using FEM car model, the defined head mass is 3.26 kg and the calculated effective head mass is 2.7 kg. The FEM model was selected for calculation of the effective head mass is because it provides more realistic head impact force.

DISCUSSION

Reconstruction of the pedestrian accident is usually much more complicated than it first appears. The interaction between a pedestrian and a car is totally different from that between an occupant and a car. Pedestrian kinematics such as wrap around trajectory, airborne trajectory, and ground landing impact could be influenced by a lot of factors such as vehicle speed, vehicle type, pedestrian anthropometrics, pedestrian posture and etc. The reliability of findings from accident reconstruction is dependent on the quality of data sources and validity of mathematical models.

ACCIDENT CASE COLLECTION: The accident data used in the current study were collected by the specialized accident investigation team. The collected accident cases provided detailed information about vehicle, pedestrian and surrounding environment at pre-crash, crash and post-crash phases. These documented information formed firm background for accident reconstructions.

Nevertheless, several uncertainties still remain for the collected accident information especially for the vehicle impact speed and initial posture of pedestrian. Calculation of vehicle speed by skid marks is the most common way in the pedestrian collision analysis and is also used in the current study. However, the skid marks only revealed the vehicle velocity at the braking moment while not at the impact moment. Usually these two moments are not coincidence. With the increasing use of Anti-lock Braking System, even skid marks are less common. The pedestrian's total throw distance is another indicator of the speed of the vehicle at impact. Several studies have revealed that the pedestrian throwing distance is correlated with the vehicle impact speed (Otte, 2004; Fugger, et al, 2002; Aronberg, 1990). Estimating vehicle speed by pedestrian throwing distance is thus becoming more important in accident investigations. It is necessary to mention that the difference of vehicle type and pedestrian anthropometric data should be counted in the calculation of vehicle impact speed by this method.

The impact responses and injury outcomes are significantly affected by the initial postures and the orientation of body segments. Therefore an appropriate initial position should be investigated and defined for reconstruction of the pedestrian accidents. In the accident investigation, these information are usually obtained by inquiring the accident witness which are objective and usually have deviations from the real condition. Another way is to use human body injuries for deducing the presumable position of the pedestrian at the moment of impact, which is proved to be more reliable (Teresinski and Madro, 2002).

PEDESTRIAN MODEL: The validity of pedestrian model is essential for the reconstruction of real world pedestrian accidents. In a study by Yang et al (2000), a MBS adult pedestrian model was developed and validated against full-scale cadaver test in terms of overall kinematics and dynamic response of various body segments. A MBS child pedestrian model was developed based on the

validated adult model and evaluated using reconstruction of real world pedestrian accident (Liu and Yang, 2002). These models are computation efficient and could provide useful information of the vehicle-human body interaction during the accident, general injury mechanism and thus are useful for the improvement of car design. However, MBS models could not provide information to investigate the injury mechanism on the tissue level. Further more, the shapes of the human bodies were represented by a group of hyper ellipsoids which is only a roughly approximation of the real human body. Facet and FEM model provide the possibility to model the human body with more complex shapes, which could result in more realistic interaction between car and body segments. With the FEM model, it is also possible to simulate the injuries on the tissue level.

The biofidelity of neck and shoulder has a great influence on the head impact response during the simulated vehicle-pedestrian collisions. In the current MBS pedestrian model, the cervical spine was simulated by an ellipsoid and linked with the head and chest by spherical joints. The joint stiffness was defined within the normal joint motion range. In a severe loading condition, the neck model may not have the sufficient biofidelity to reproduce the real neck motion. The shoulder joint was defined by a spherical joint. Neale et al (2003) compared the JARI pedestrian model and TNO pedestrian model with the cadaver tests and found both two models had a poor shoulder biofidelity. The current shoulder model has limitation to simulate the deformations and compressions of the shoulder under severe loading conditions. Further development of the neck and shoulder models is necessary to obtain more realistic head impact behaviour.

VEHICLE MODEL: The validity of vehicle model is also the prerequisite for the accident reconstruction. The shapes of vehicle front could usually obtained from production car drawings and modeled by hyper ellipsoids or meshes. The mechanical property of the vehicle is another important parameter. The mechanical properties could be derived from the acceleration history information of the impactor test. To achieve the correct calculated injury parameters, it requires the subsystem impact tests be conducted at precisely the same impact point as in the accident and on the same car model as the accident car. However, for large-scale accident reconstructions it is quite expensive and time consuming to conduct such impact test for all the cases.

EuroNCAP evaluated the pedestrian safety of current production cars according to EEVC test procedures. A series of impactor tests have been carried out to replicate accidents involving child and adult pedestrians where impacts occur at 40 km/h. For each tested car, it is possible to obtain the stiffness corridors for windscreen, hood, hood edge and bumper. These corridors could be used in the reconstructions instead of a single force-deformation curve at the impact location. Nevertheless, due to the use of stiffness corridor, the resulting calculated injury parameter values are also corridors.

NUMERICAL METHODS: Three different numerical methods are used in the current study. The overall kinematics of child pedestrians are quite similar to each other and correspond well to the dents found on the accident car (Figure 6). The calculated throw distance and wrap around distance in each reconstruction is also close to the values in the accident, as listed in Table 1.

As for the head impact condition, each reconstruction has the similar impact timing and impact velocity. Variation appears for the head impact angle. The MBS model has the smallest impact angle of 60° while the facet model has the largest impact angle of 84° as shown in Figure 7. The reason may be that the FEM model provided more realistic deformation pattern of the vehicle hood compared with the large penetration of the pedestrian body into the hood in the MBS and facet models.

Table 2 shows the calculated head injury parameters and these values are on the same level. The time histories of head acceleration from different numerical simulations are quite similar as shown in Figure 8. However, noticeable variations of these values from the three computer models still exist despite the fact that each model could replicate the kinematics of the child during the accident. Considerably more work is required to understand the reasons for the differences in the results with a view to, in due purpose, settling on one model to guide the further study.

INJURY BIOMECHANICS: The head injury mechanism especially for the children remained unclear due to the scarce of the experimental data. The injury criteria and threshold used today are derived from the available adult data by using scaling method. Reconstruction the real world child

pedestrian accident and correlate the calculated head injury parameters with the head injury outcomes provided a possible way to understand the head injury mechanism of children and evaluate current injury criteria and thresholds.

NHTSA proposed HIC_{15} of 700 as an injury limit for a 6-year-old child dummy (Eppinger, 1999), which is derived based on the scaling method. In the example case, the child sustained fracture at left orbit (AIS 3), subdural hematoma at left frontal lobe (AIS 5). The mean values of the calculated head injury parameters are listed in Table 2. The mean value of HIC_{15} is 1520 which corresponds well with the injury outcome according to the above injury criteria.

CONCLUSION

The MBS model is quite efficient and accurate for reconstructing the pedestrian accident when investigating the influence of the car front shape and general injury mechanism. Facet model and FEM model provided more precise vehicle front shape modelling and thus believed to inprove the accuracy of the results. However, the later two methods increase both the modelling time and computing time.

The reconstruction results are useful to understand the influence of vehicle front structure on the resulting injury severity and thus to improve the car front design. By correlating the calculated injury parameters with the injury outcomes, it is also able to understand the child pedestrian injury mechanism which is impossible to accquire from the biomechanical test due to ethical reasons.

To account for the influence of neck restraint on the head during the pedestrian accident, the headform test conditions and injury criteria should be adjusted. Further research is needed in this area.

ACKNOWLEDGMENTS

This study was sponsored by the European Community under the TIP3-CT-2004-506503 APROSYS project.

REFERENCE

Al-Ghamdi, A. S., Pedestrian-vehicle crashes and analytical techniques for stratified contingency tables. Accident Analysis & Prevention 34(2), 2002, pp. 205-214

Aronberg, R., Airborne trajectory analysis derivation for use in accident reconstruction. SAE paper, No. 900367, 1990

Berg, F. A., Egelhaaf, M., Bakker, J., Bürkle, H., Herrmann, R., Scheerer, J., Pedestrian Protection in Europe- The Potential of Car Design and Impact Testing, Report for United Nations Economic Commission for Europe, www.unece.org/trans/doc/2002/wp29grsp/inf-gr-ps-12e.pdf, accessed March 31, 2005.

CARE – (http://europa.eu.int/comm/transport/home/care/index_en.htm), Community database on Accidents on the Roads in Europe, 2004

EEVC Working Group 17- Improved Test Methods to Evaluate Pedestrian Protection Afforded by Passenger Cars, 2002

Eppinger, R., Sun, E., Bandak, F. , et al, Development of Improved Injury Criteria for the Assessment of Advanced Automotive Restraint Systems – II. NHTSA Technical Report, 1999

FARS- National Highway Traffic Safety Administration's (NHTSA) Fatality Analysis Reporting System (FARS) Web-Based Encyclopedia, http://www-fars.nhtsa.dot.gov/, 2004

FARS- National Highway Traffic Safety Administration's (NHTSA), Fatality Analysis Reporting System (FARS) Web-Based Encyclopaedia, http://www-fars.nhtsa.dot.gov/, 1995-2002

Fildes, B., Gabler, H.C., Otte, D., Linder, A., Sparke, L., Pedestrian impact priorities using real-world crash data and harm. Proceeding of 2004 IRCOBI conference, Austria, 2004

Fugger, T.F., Randels, B.C., Wobrock, J.L., Eubanks, J.J., Pedestrian Throw kinematics in forward projection collisions. SAE paper, No. 2002-01-0019, 2002

IHRA - International Harmonized Research Activities, Pedestrian Safety Working Group 2001 Report, 2001.

JTSP - Japan Traffic Safety Policy Office Management and Coordination Agency, White paper on traffic safety in Japan. Tokyo, Japan, 2003.

Liu, X.J and Yang, J.K. Development of Child Pedestrian Mathematical Models and Evaluation with Accident Reconstruction, Traffic Injury Prevention, 2002, 3(4):321-329.

Neale, M.S., Hardy, B.J., Lawrence, G.J.L., Development and review of the IHRA (JARI) and TNO pedestrian models, Proc. of 18th ESV conference, 2003

Otte, D., Severity and Mechanism of Head Impacts in Car to Pedestrian Accidents, Proc. of Int. IRCOBI Conf. Biomechanics Impacts, 1998, pp.329-341.

Rivara, F.P. Child Pedestrian Injuries in the United States: Current Status of the Problem, Potentential Interventions, and future Research Needs. AJDC, 1990, 144:692-6

Teresinski, G., Madro, R., Evidential value of injuries useful for reconstruction of the pedestrian–vehicle location at the moment of collision, Forensic Science International, Volume 128, Issue 3, 2002, pp. 127-135.

TNO-MADYMO Utilities Manual. Version 6.1, Road-Vehicle Research Institute, Delft, The Netherlands, 2003.

Yang, J, Effects of Vehicle Front Design Parameters on Pedestrian Head-Brain Injury Protection, The 18th ESV Conference 19-22 May, 2003, in Nagoya, Japan.

Yang, J. K., Lövsund P., Cavallero, C., and Bonnoit, J, A human-body 3D mathematical model for simulation of car-pedestrian impacts, Journal of crash prevention and injury control, 2(2), 2000 pp.131-149.